SEMARAK ILMU PUBLISHING

Journal of Advanced Research in Fluid Mechanics and Thermal Sciences

Journal homepage:
https://semarakilmu.com.my/journals/index.php/fluid_mechanics_thermal_sciences/index
ISSN: 2289-7879

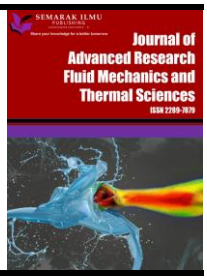

Hyperbolic Tangent Fluid Model for Stagnation Flow of Hybrid Nanofluid Over a Stretching Sheet

Zaileha Md Ali[1], Nur Zahidah Ismail[1], Mohd Rijal Ilias[1], Siti Khuzaimah Soid[1,*], Anuar Ishak[2], Md Faisal Md Basir[3], Nur Hazirah Adilla Norzawary[4]

[1] School of Mathematical Sciences, College of Computing, Informatics and Media, Universiti Teknologi MARA, 40450 Shah Alam, Selangor, Malaysia
[2] School of Mathematical Sciences, Faculty of Science and Technology, Universiti Kebangsaan Malaysia, 43600 Bangi, Selangor, Malaysia
[3] Faculty of Science, Universiti Teknologi Malaysia, 81310 Skudai, Johor, Malaysia
[4] Institute for Mathematical Research (INSPEM), Universiti Putra Malaysia, 43400 Serdang, Selangor, Malaysia

ARTICLE INFO

Article history:
Received 12 February 2023
Received in revised form 23 May 2023
Accepted 30 May 2023
Available online 19 June 2023

Keywords:
Hybrid nanofluid; hyperbolic tangent fluid model; stretching sheet; boundary layer; radiation; stagnation point flow

ABSTRACT

The problem of hyperbolic tangent fluid model for stagnation flow of hybrid nanofluid over a stretching sheet is investigated. Constitutive relation of an incompressible hyperbolic tangent model as well as consideration of thermal radiation and Newtonian heating is taken into account. The boundary layer problem is formulated to nonlinear partial differential equations which is then transformed into ordinary differential equations by using similarity transformation. The equations including the boundary conditions are solved numerically using bvp4c in the MATLAB software. A comparison with previous findings shows an excellent agreement. The effect of governing parameters such as power law index, Weissenberg number, suction/injection, radiation and Biot number is investigated. The changes in the value of volume fraction of diamond and silicon dioxide are also analyzed. Characteristics for the significant variables are graphically presented and the numerical results are tabulated. The velocity behavior is significantly influenced by the volume fraction of diamond and silicon dioxide and other physical parameters. Meanwhile, the temperature is influenced by the radiation parameter. This study provides conclusive evidence that increasing the volume fraction of diamond nanoparticles significantly enhances the heat transfer rate. The increment by 0.1 (10%) of the volume fraction of diamond nanoparticles increases the heat transfer rate approximately by 3%. These findings underscore the potential of integrating these nanoparticles to improve thermal performance across diverse applications.

1. Introduction

In 1904, Prandtl revolutionized the concept of boundary layers by introducing a new understanding and analysis of fluid dynamics. His theory emphasizes that the fluid instantly adjacent to the surface caused by the frictional effects with a no-slip condition in a boundary layer [1]. Heat transfer is a crucial technical process in many industrial and engineering sectors. Heat transfer is also

* *Corresponding author.*
E-mail address: khuzaimah@tmsk.uitm.edu.my

https://doi.org/10.37934/arfmts.107.1.87101

known as a result of the change in temperature between the conversions of energy from one form to another form [2].

The study of the boundary layer, particularly under stretching surface conditions, provides valuable insights into the fluid dynamics and heat transfer phenomena that occur in various engineering applications. There are crucial applications on the stretching plate especially in manufacturing and industrial such as in the performance of lubricants, the movement of biological, the cooling of metallic plates and the plastic sheet extrusion [3]. A large amount of work through different stretching velocities, situations and models in this direction has been reported [4-9].

The exploration of boundary layer and heat transfer phenomena in nanofluids yields valuable insights into the behaviour and performance of these sophisticated fluid systems. By comprehending the intricate interplay between the boundary layer, heat transfer mechanisms, and the unique properties of nanofluids, we can facilitate the advancement of efficient thermal management systems, enhance heat transfer rates, and optimize the overall performance of diverse nanofluid-based applications. Nanofluid is a new admixture fluid as stated in Choi's theory [10]. Based on Choi's theory, nanofluid is formed by adding nanoparticles into the base fluid. Choi also stated that by comparing the base fluid to the nanofluids, the nanofluids have higher thermal conductivity to enhance heat transfer behaviour. The study of nanofluids' properties has been extensively investigated since its broad applications in industrial engineering especially cooling, heat exchangers, food, double pane windows, transportation, and biomedicine. A comprehensive study of current and future nanofluids applications has been explored by Wong and Leon [11]. Numerous researchers have studied the fluid flow and heat transfer over a range of geometric figures such as a flat surface, cone, cylinder, and other shapes numerically [12-14].

According to the literature, Soid *et al.,* [15] studied the laminar forced convection boundary layer flow along a horizontal thin needle. The results are generated by a boundary value problem 4C solver (BVP4C). They stated that dual solutions exist when the needle and the free stream move in opposite directions. Moreover, the investigation of stagnation-point flow is an vital topic in fluid mechanics when a flow impinges perpendicularly to a solid surface in which the shear stress is zero. It has engaged the interest of many researchers due to its industrial applications such as flows over the tips of aircraft wings and submarines [16,17]. Othman *et al.,* [18] explored a stagnation point flow in a mixed convection boundary layer over a vertical plate immersed in a nanofluid. They solved the problem numerically by shooting method and they found the increament in the mixed convection parameter tends to increase the mass transfer, skin friction coefficient and heat rates at the plate. Moreover, they also discovered a unique solution for stretching and dual solutions for shrinking plates. Recently, there are many similar types of research focusing on this topic in various aspects of parameters immersed in a nanofluid [19-24].

In the study of both boundary layer and stagnation point flow, it is essential to investigate both traditional nanofluids and hybrid nanofluids, as they represent significant areas of exploration and research. The composition of nanoparticles by two or more different materials of nanometer size in a based fluid is defined as a hybrid nanofluid that attains a synergistic effect [25,26]. Extensive research has shown a significant improvement in the heat conductivity of this novel fluid, as seen in studies by Arani and Aberoumand [27] where they consider stagnation hybrid nanofluid flow of silver-copper oxide (Ag-CuO) and water over a slippery stretching and shrinking sheet. The coefficient of skin friction and the rate of Nusselt number of the hybrid nanofluids increase with the inclusion of suction and injection parameters. The problem of stagnation-point flow in hybrid nanofluid has been extended in numerous ways including various shapes and physical effects such as Khan *et al.,* [28], Gul *et al.,* [29], Wahid *et al.,* [30], Saupi *et al.,* [31], Khashi'ie *et al.,* [32] and Zainal *et al.,* [33].

Besides, a fluid where its stress and rate of deformation have variable proportionality is known as a non-Newtonian fluid which is described by Sir Isaac Newton [34]. The resistance of fluid against the exerting of the shear stress changes with the variation rate of the material length is defined as the non-Newtonian fluids [35]. The hyperbolic tangent model is a rheological model that possesses many significant values as compared to other non-Newtonian formulations which are absent of complication, physical stability, and smooth of computation. Hayat *et al.,* [36] investigated influence of thermal radiation in MHD stagnation point flow towards an exponentially stretching sheet is where incompressible hyperbolic tangent liquid is taken into account. They concluded that heat transfer rate for larger Prandtl number, Biot number and radiation factor is higher when compared with Eckert number. Following them, the research about hyperbolic tangent models has studied by many researches and become the core of some applications in the engineering and medical fields [37-40].

After reviewing the existing literature, we are inspired by the work of Hayat *et al.,* [36]. Therefore, we want to improve their model by implementing Newtonian heating, including hybrid nanofluid thermophysical properties as well as constant suction/injection effects on the boundary conditions [41,42]. Furthermore, we also want to include the effect of radiation, and suction/injection due to its powerful impact on the fluid flow and heat transfer together with other governing parameters over an exponentially stretching permeable sheet using the hyperbolic tangent fluid model for hybrid nanofluid over a stretching surface [43,44]. It is generally known that radiation and suction/injection parameter can alter and control the fluid dynamic system, hence, the implementation of those parameters are emphasized and considered in this study. Diamond and silicon dioxide are considered as the nanoparticles. The combination of diamond and silicon dioxide as hybrid nanoparticles is advantageous due to their complementary properties. Diamond nanoparticles possess exceptional thermal conductivity, mechanical strength, and chemical stability [45]. Silicon dioxide nanoparticles, on the other hand, offer good dispersibility, surface functionalization capabilities, and compatibility with various matrices. By merging these materials, the resulting hybrid nanoparticles inherit the diamond's thermal properties and silicon dioxide's versatility. This synergy enables enhanced heat transfer, improved dispersion, and diverse applications in electronics, thermal management, and biomedicine.

The main goal of this study is to (i) formulate the appropriate model, (ii) solve the model using the numerical method, (iii) generate the numerical findings in the form of data and graphs, and (iv) analyze and discuss the findings accordingly in terms of the impact of parameters towards the fluid flow and heat transfer properties.

2. Methodology

Consider a steady radiative stagnation of laminar hybrid nanofluid flow using hyperbolic tangent fluid model towards an exponentially stretching permeable surface with Newtonian heating is investigated depicted in Figure 1.

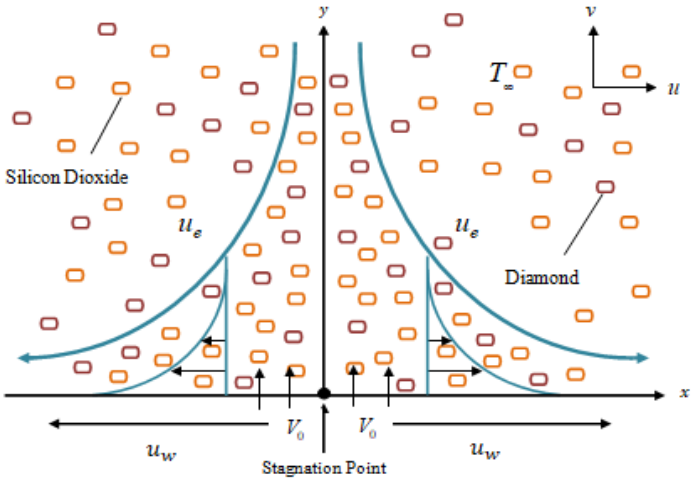

Fig. 1. Physical configuration of the problem for stretching surface

The governing boundary layer parabolic partial differential equations (PDEs) are written as [36]

$$\frac{\partial u}{\partial x}+\frac{\partial v}{\partial y}=0 \tag{1}$$

$$u\frac{\partial u}{\partial x}+v\frac{\partial u}{\partial y}=\nu_{hnf}(1-n)\frac{\partial^2 u}{\partial y^2}+\sqrt{2}\nu_{hnf}n\Gamma\frac{\partial u}{\partial y}\frac{\partial^2 u}{\partial y^2}+u_e\frac{du_e}{dx} \tag{2}$$

$$u\frac{\partial T}{\partial x}+v\frac{\partial T}{\partial y}=\left[\frac{k_{hnf}}{(\rho C_p)_{hnf}}+\frac{16\sigma_1 T_\infty^3}{3(\rho C_p)_{hnf}k_1}\right]\frac{\partial^2 T}{\partial y^2} \tag{3}$$

along with the initial and boundary conditions

$$\begin{aligned} &u=u_w=U_0e^{\left(\frac{x}{L}\right)},-k_{hnf}\frac{\partial T}{\partial y}=h_sT,\text{at } y=0\\ &u\to u_e=U_\infty e^{\left(\frac{x}{L}\right)} \text{ as } y\to\infty \end{aligned} \tag{4}$$

where u is the component velocity along x-axis, v is the component velocity along y-axis, n is the power law index, ν_{hnf} is the kinematic viscosity of the hybrid nanofluid, u_e is the free stream velocity, k_{hnf} is the thermal conductivity of the hybrid nanofluid, $(\rho C_p)_{hnf}$ is the heat capacity of the hybrid nanofluid, σ_1 is the Stefan Boltzmann constant, and k_1 is the Rosseland mean absorption coefficient and $h_s=he^{\left(\frac{x}{2L}\right)}$ is the convective heat transfer coefficient.

Then the subsequent similarity variables can be regarded for Eq. (1) to Eq. (3)

$$\eta=\sqrt{\frac{U_0}{2\nu_{bf}L}}e^{\left(\frac{x}{2L}\right)}y,\ u=U_0e^{\left(\frac{x}{L}\right)}f'(\eta),\ v=-\sqrt{\frac{\nu_{bf}U_0}{2L}}e^{\left(\frac{x}{2L}\right)}[f(\eta)+\eta f'(\eta)],\ \theta(\eta)=\frac{T-T_\infty}{T_\infty} \tag{6}$$

where η is the similarity variable, U_0 is the reference velocity, v_{bf} is the kinematic viscosity of base fluid and θ is the dimensionless temperature. Replacing (6) into Eq. (1) to Eq. (4), we retrieve the following differential equations

$$\frac{P_1}{P_2}(1-n)f''' - 2f'^2 + ff'' + \frac{P_1}{P_2}nWef''f''' + 2A^2 = 0 \tag{7}$$

$$\left[P_4 + \frac{4}{3}R_d\right]\theta'' + P_3 Prf\theta' = 0 \tag{8}$$

along with the boundary conditions

$$\begin{aligned} &f'(\eta) = 1, f(\eta) = S,\ \theta'(\eta) = -\gamma[\theta(\eta)+1], at\ \eta = 0 \\ &f'(\eta) \to A, \theta(\eta) \to 0 \text{ as } \eta \to \infty \end{aligned} \tag{9}$$

where $P_1 = \frac{\mu_{hnf}}{\mu_{bf}}$ is dynamic viscosity, $P_2 = \frac{\rho_{hnf}}{\rho_{bf}}$ is density, $P_3 = \frac{(\rho C_p)_{hnf}}{(\rho C_p)_{bf}}$ is heat capacity and $P_4 = \frac{k_{hnf}}{k_{bf}}$ is thermal conductivity of the hybrid nanofluids, $f(\eta)$ is the dimensionless stream function, We is the Weissenberg number, A is the ratio of velocities, Pr is the Prandtl number, R_d is the radiation parameter, S is the suction/injection parameter, and γ is the conjugate parameter for Newtonian heating, which are defined as

$$We = \frac{U_0^{3/2}\Gamma e^{\left(\frac{3x}{2L}\right)}}{\sqrt{v_{bf}L}},\ A = \frac{U_\infty^2}{U_0^2},\ Pr = \frac{\mu_{bf}(C_p)_{bf}}{k_{bf}},\ R_d = \frac{4\sigma_1 T_\infty^3}{k_1 k_{bf}},\ S = -\frac{V_0}{\sqrt{\frac{v_{bf}U_0}{2L}}},\ \gamma = \frac{h}{k_{hnf}}\sqrt{\frac{2v_{bf}L}{U_0}} \tag{10}$$

The subscript 1 and 2 indicate the physical properties of diamond and Silicon Dioxida (SiO_2) respectively. The total volume concentration of both nanoparticles are denoted by ϕ given as $\phi = \phi_1 + \phi_2$. The thermophysical properties of the hybrid nanofluid and nanoparticles are presented in Table 1 and Table 2, respectively.

Table 1
Thermophysical properties of hybrid nanofluids [46]

Properties	Hybrid Nanofluids
Dynamic Viscosity (μ)	$\mu_{hnf} = \frac{\mu_{bf}}{\left[1-(\phi_1+\phi_2)\right]^{2.5}}$
Density (ρ)	$\rho_{hnf} = \left[\phi_1\rho_{s1} + \phi_2\rho_{s2} + (1+\phi)\rho_{bf}\right]$
Heat Capacity (ρC_p)	$(\rho C_p)_{hnf} = \left[\phi_1(\rho C_p)_{s1} + \phi_2(\rho C_p)_{s2} + (1-\phi)(\rho C_p)_{bf}\right]$
Thermal Conductivity (k)	$\frac{k_{hnf}}{k_{bf}} = \frac{\phi_1 k_{s1} + \phi_2 k_{s2} + 2\phi k_{bf} + 2\phi(\phi_1\rho_{s1} + \phi_2\rho_{s2}) - 2\phi^2 k_{bf}}{\phi_1 k_{s1} + \phi_2 k_{s2} + 2\phi k_{bf} - \phi(\phi_1\rho_{s1} + \phi_2\rho_{s2}) + \phi^2 k_{bf}}$

Table 2
Thermophysical values of base fluid and nanoparticles [47]

Properties	Diamond (ϕ_1)	Silicon Dioxide, SiO_2 (ϕ_2)	Sodium Alginate ($C_6H_9NaO_7$)
$\rho(kg/m^3)$	3510	2650	989
$C_p(J/kgK)$	497.26	730	4175
$k(W/mK)$	1000	1.5	0.613

The involved physical quantities are the skin friction coefficient C_f and the local Nusselt number Nu_x

$$C_f = \frac{\tau_w}{\rho u_w^2}, Nu_x = \frac{xq_w}{k_{bf}(T-T_\infty)} \tag{11}$$

Using the similarity variables (6) then

$$\begin{aligned} Re_x^{1/2} C_f &= \frac{P_1}{P_2}\sqrt{\frac{1}{2L}}\left[(1-n)f'' + \frac{n}{2}Wef''^2\right] \\ Re_x^{-1/2} Nu_x &= -x\sqrt{\frac{1}{2L}}\left[\left(P_4 + \frac{4}{3}R_d\right)\frac{\theta'}{\theta}\right] \end{aligned} \tag{12}$$

where $Re_x^{1/2} = \sqrt{\frac{U_0}{\nu_{bf}} e^{\left(\frac{x}{2L}\right)}}$ is the local Reynolds number.

3. Results

The transformed non-linear boundary layer equations were solved numerically by using bvp4c in MATLAB software. The values of the skin friction were computed for various values velocity ratio A with other parameters were set to be constant at $n = We = R_d = S = 0$ and $P_1 = P_2 = P_3 = P_4 = 1$. Table 3 shows the comparison of the skin friction coefficient $f''(0)$ between the results obtained from Mustafa *et al.,* [48] using the homotopy analysis method (HAM) and Hayat *et al.,* [36] using the bvp4C solver with the present study. The numerical results stated are in an excellent agreement. Therefore, this verifies the reliability and accuracy of the method in this study. It is noticed that the values of the magnitude of the skin friction coefficient $f''(0)$ decreases as A increases. The negative value indicates the drag force exerts from the surface to the fluid.

Table 3
Comparison for numerical values $f''(0)$ for $A = 0.0, 0.1, 0.2, 0.5, 0.8, 1.2$

A	Mustafa *et al.,* [48]	Hayat *et al.,* [36]	Present Study
0.0	-1.281809	-1.281809	-1.28180857
0.1	-1.253580	-1.253580	-1.25357990
0.2	-1.195120	-1.195118	-1.19511787
0.5	-0.879835	-0.879833	-0.87983365
0.8	-0.397771	-0.397767	-0.39777179

The numerical values of the skin friction coefficient and the rate of heat transfer are tabulated in Table 4 for both suction $S=0.5$ and injection $S=-0.5$ with fixed values of volume fraction of silicon dioxide $\phi_2=0.1$, power law index $n=0.2$, ratio of velocity $A=0.1$, Weissenberg number $We=0.5$, Prandtl number $\Pr=6.45$, radiation parameter $R_d=0.3$, and Biot number $y=0.2$. It is found as ϕ_1 increases, the magnitude of drag force $\left|f''(0)\right|$ decreases for both suction and injection effects. The decrement of drag force reflects that the hybrid particles of the fluid flows move quite smoothly on the surface for every increment of ϕ_1. Apparently, the surface exerts a drag force to the fluid that causes movement on the surface due to the negative value. Furthermore, the heat disperses more for a higher percentage of diamond volume fraction specifically when the fluid is sucked on the surface. However, the analysis contradicts when less heat is transferred for a higher percentage of diamond as the fluid is injected to the surface. Moreover, the heat transmitted from the surface to the fluid is rectified by the positive Nusselt number. Hence, the results are consistent with graphical illustrations in Figure 2 and Figure 3.

Table 4
Values of the skin friction coefficient and the heat transfer rate for diamond volume fraction ϕ_1 on the velocity profiles when $n=0.2, A=0.1, We=0.5, Pr=6.45, R_d=0.3$ and $y=0.2$

ϕ_1	ϕ_2	S	$f''(0)$	$-\theta'(0)$
0.0	0.1	0.5	-1.26855514	0.21469981
0.1	0.1		-1.26350276	0.22130834
0.2	0.1		-1.18984161	0.22745000
0.0	0.1	-0.5	-0.94820936	0.45381841
0.1	0.1		-0.94535082	0.43600493
0.2	0.1		-0.90306366	0.43648263

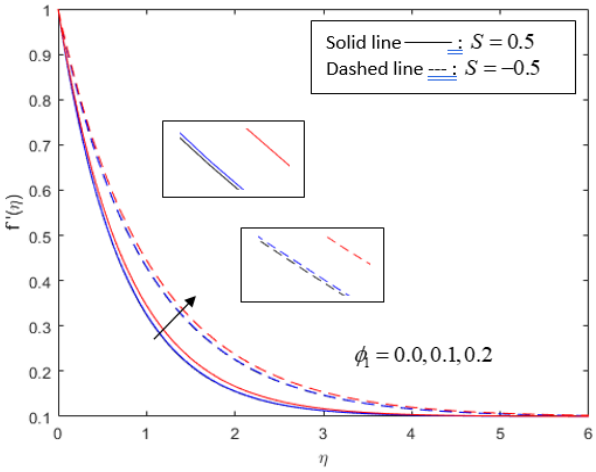

Fig. 2. Effects of various values of volume fraction (ϕ_1) on velocity profiles

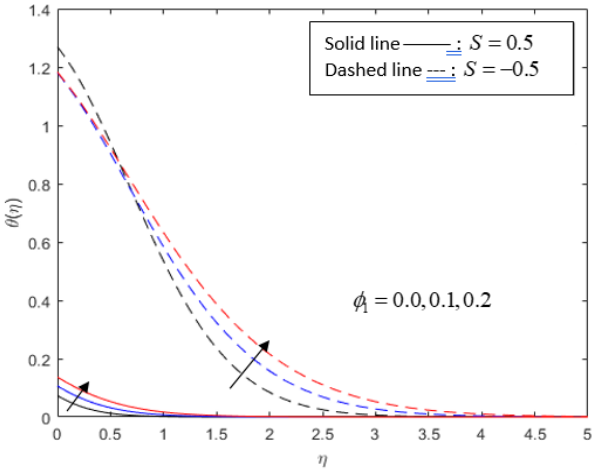

Fig. 3. Effects of various values of volume fraction (ϕ_1) on temperature profiles

Figure 2 and Figure 3 also show the behavior of velocity and temperature of the fluid in the boundary layer when the volume fraction of diamond ϕ_1 increases in the presence of suction/injection respectively. Noticeably, the velocity of the fluid in the boundary layer increases with the existence of diamond ϕ_1. Both cases have a similar pattern of velocity profiles, this is due to the physical reason that the diamond nanoparticles affect the boundary layer by interacting with fluid molecules, increasing its thickness, and slowing down the transition from high-velocity to slower-

moving fluid near the solid surface. Their small size and high surface area facilitate efficient mixing and dispersion, resulting in enhanced fluid velocity.

The temperature profile in Figure 3 increases as ϕ_1 increases in the presence of suction while for injection, the temperature decreases at the beginning then increases as ϕ_1 increases. This phenomenon happens due to the nature of the surface which the injected fluid to the surface leading to unstable flow that results in decreasing the rate of heat transfer on the surface. This shows that the behavior of the temperature in Figure 3 is affected differently by the increment of ϕ_1 in the presence of suction and injection. As a consequence of the increment of the temperature, the thickness of the thermal boundary layer significantly increases as well. Hence, this implies that the cooling down for the temperature of the fluid is delayed as ϕ_1 increases.

Figure 4 and Figure 5 show the effect on the velocity and the temperature profiles when the volume fraction of silicon dioxide (ϕ_2) increases in the presence of suction/injection. The results are consistent with Figure 2 and Figure 3 where the velocity and the temperature behaviors increase as ϕ_2 increases as well as the velocity and thermal boundary layer thicknesses are thicker for injection case. The same physical reasoning as Figure 2 and Figure 3 also applies to this behavior since silicon dioxide also has a high surface area due to its nanometer size.

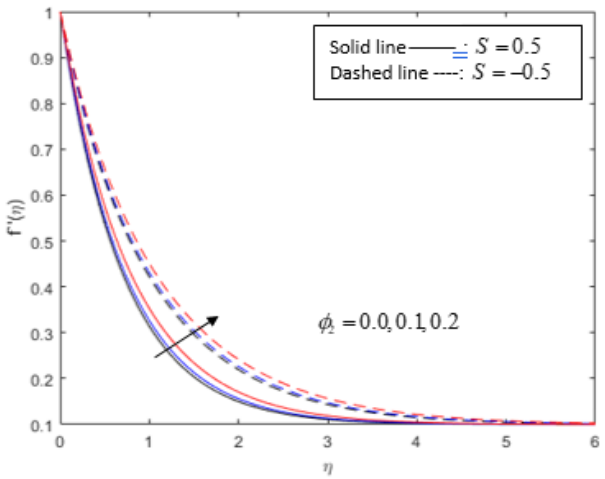

Fig. 4. Effects of various values of volume fraction (ϕ_2) on velocity profiles

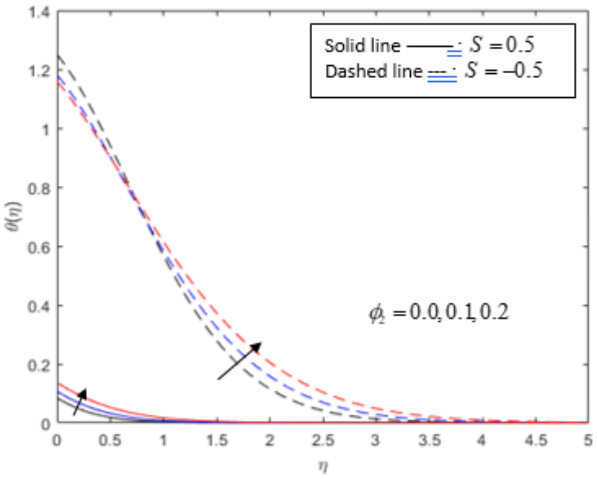

Fig. 5. Effects of various values of volume fraction (ϕ_2) on temperature profiles

Table 5 explains the influence of the suction $(S>0)$ and injection $(S<0)$ effects with ratio between 0.5 and 2.0 on the skin friction coefficient $f''(0)$ and the rate of heat transfer $-\theta'(0)$. The absolute value of skin friction and the rate of heat transfer show increment and decrement behavior on the surface, respectively. An opposite phenomenon of the drag force occurs when the injection is imposed on the surface. Similarly, a consistent behavior occurs when the heat is dispersed at the surface. Physically as $S=-0.5$, the heat is dominantly transmitted from surface to fluid. Surprisingly, a reverse phenomenon happens when injection reaches -1.0. Moreover, as a greater injection is imposed on the surface, then the heat is transferred gradually from fluid to surface as implicated by the insignificant negative value of the Nusselt number.

Table 5
Values of the skin friction coefficient and the heat transfer rate for various values of suction $(S>0)$ and injection $(S<0)$ on velocity profiles when $n=0.2, A=0.1, We=0.5, \Pr=6.45, R_d=0.3$ and $y=0.2$

S	$f''(0)$	$-\theta'(0)$
0.5	-1.26350276	0.22130834
1.0	-1.45549816	0.21325802
1.5	-1.66396511	0.20945137
2.0	-1.88352699	0.20728816
-0.5	-0.94535082	0.43600493
-1.0	-0.82163177	-0.07199637
-1.5	-0.71913486	-0.00169009
-2.0	-0.63455774	-0.00000693

In the boundary layer, the velocity of the fluid decreases as the suction $(S>0)$ increases shown in Figure 6 while Figure 7 shows the temperature distribution decreases. This can be physically true because, logically, as suction is increased, the fluid velocity decreases due to pressure drops and flow restrictions. Also, suction can induce heat transfer from the fluid to colder surfaces or mediums, resulting in a reduction in fluid temperature. The velocity of the fluid increases as the injection $(S<0)$ increases illustrated in Figure 8 but Figure 9 shows a non-uniform temperature distribution. Obviously, there exists an isolated behavior for $S=-0.5$ where its surface temperature profile is in negative gradient $\theta'(0)$. Consequently, both thicknesses of the velocity and thermal boundary layer decrease for suction and vice versa for injection. This can be physically deduced that suction reduces the thickness of the boundary layer by extracting fluid from the surface, resulting in thinner boundary layers. In contrast, injection increases the thickness of the boundary layer by introducing additional fluid near the surface, leading to thicker boundary layers.

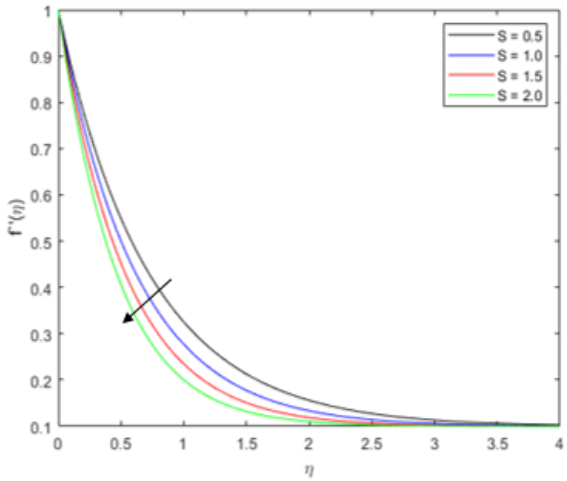

Fig. 6. Effects of various values of suction $(S>0)$ on velocity profiles

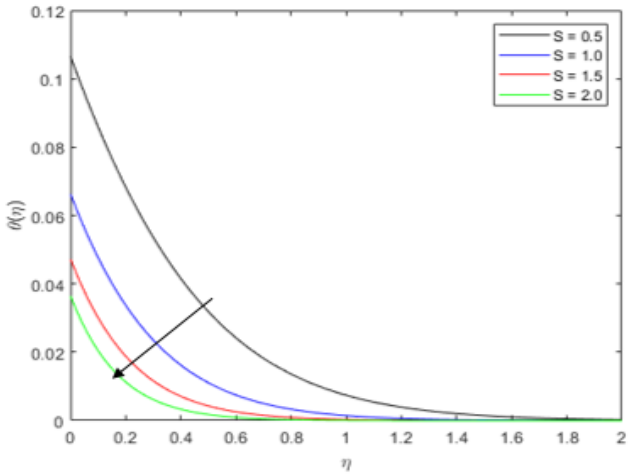

Fig. 7. Effects of various values of suction $(S>0)$ on temperature profiles

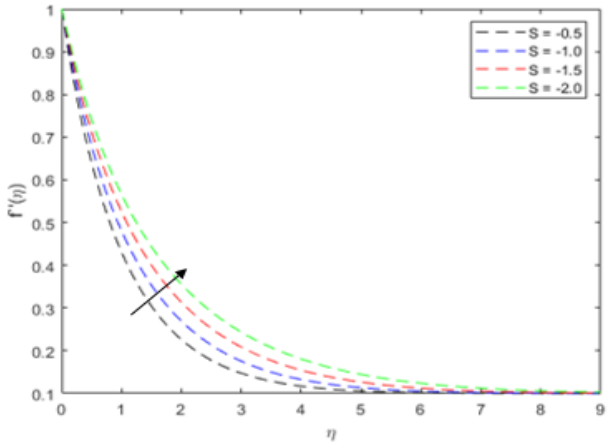

Fig. 8. Effects of various values of injection $(S<0)$ on velocity profiles

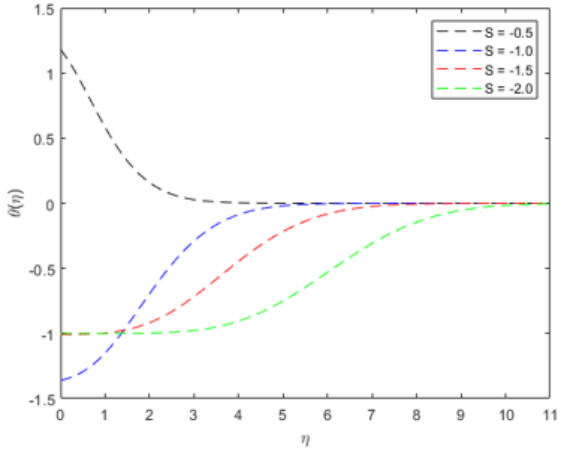

Fig. 9. Effects of various values of injection $(S<0)$ on temperature profiles

Figure 10 explains the impact of the power law index on the velocity distribution with the presence of both suction and injection on the stretching surface. The velocity profile increases for larger n in the presence of suction/injection and consequently the thickness of the boundary layer also increases. Substantially, the fluid shows its shear thinning behavior $(n<1)$ which in return gives lower viscosity and consequently velocity $f'(\eta)$ grows. However, opposite results are observed in Newtonian fluid as reported by Hayat *et al.,* [36]. The enhancement of the velocity may due to the addition of the thermophysical properties of the hybrid nanofluid. Meanwhile, Figure 11. shows the temperature decreases slightly as n increases in the presence of suction as compared to those in the presence of injection. This indicates that as n increases, the injection affects the behavior of temperature more than suction. Apparently, both values of the skin friction and the rate of heat transfer decrease as n increases in the presence of suction/injection. The drag force is dominant when the fluid is sucked to the surface but the heat transfer process on the surface is not as significant.

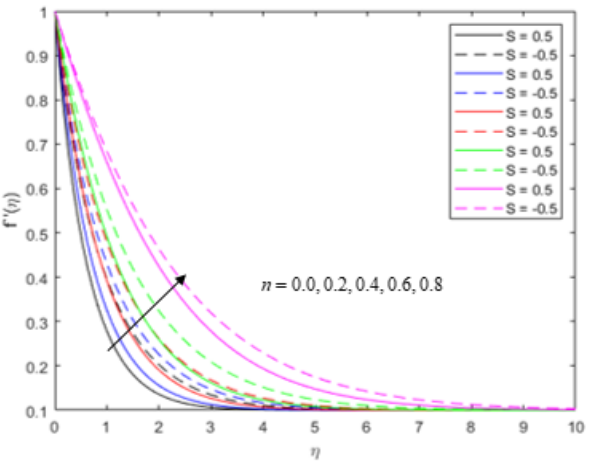

Fig. 10. Effects of various values of power law index (n) on velocity profiles

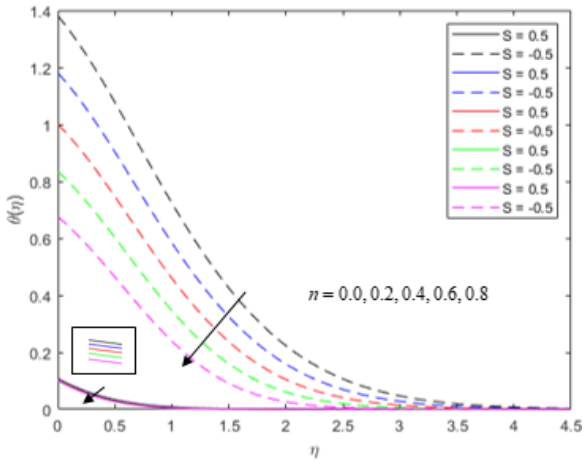

Fig. 11. Effects of various values of power law index (n) on temperature profiles

Weissenberg number defines the relaxation time ratio of the fluid as well as the relaxation time of the shear rate. The rise in the Weissenberg number as shown as in Figure 12 and Figure 13 increases the velocity profile and decreases the temperature profile for both suction/injection.

Consequently, thickens the velocity boundary layer thickness, while diminishes the thermal boundary layer thickness. Similar observations on the skin friction and the Nusselt number are achieved for the Weissenberg number as in the power law index for both suction and injection. Hence, Figure 12 and Figure 13 have a similar pattern as in Figure 10 and Figure 11.

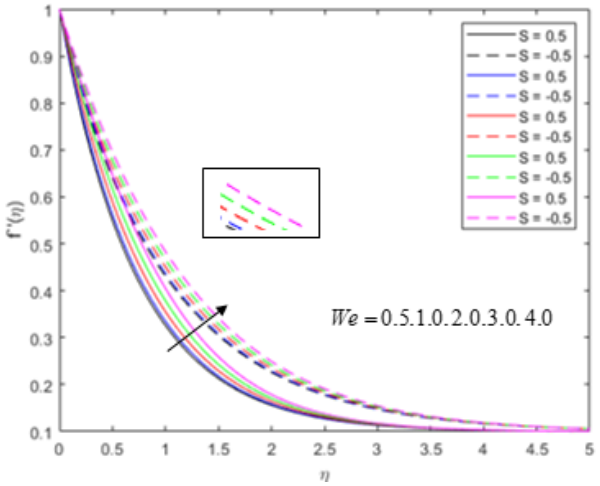

Fig. 12. Effects of various values of Weissenberg number (We) on velocity profiles

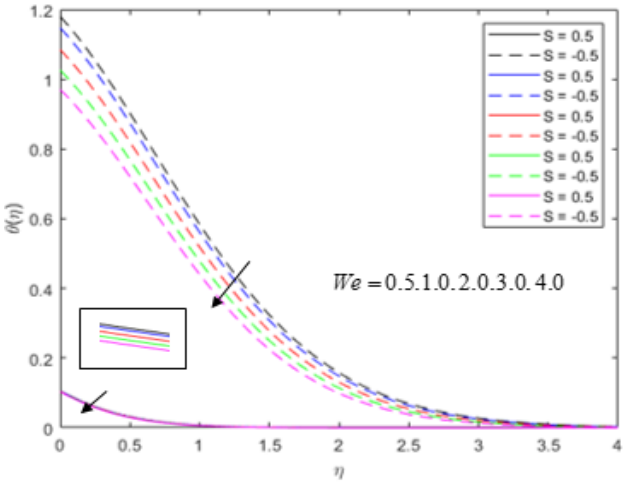

Fig. 13. Effects of various values of Weissenberg number (We) on temperature profiles

Figure 14 shows the temperature increases as (R_d) increases with the presence of suction/injection. This implies the thickness of the thermal boundary layer also increases since the higher value of the radiation parameter (R_d) gives more heat to the working fluid. The velocity profile remains unchanged since radiation does not affect the fluid flow as proven in the momentum Eq. (2). Furthermore, Figure 15 depicts the Biot number (y) does affect the temperature distribution especially in the presence of injection. The fluid temperature in the boundary layer increases as y increases and gradually the thickness of the thermal boundary layer increases. However, the temperature distribution decreases for $y = 0.4$ and then increases again when $y = 0.5$ and 0.7. The imbalanced fluid temperature in the boundary layer may be caused by the surface heat transfer coefficient h_s together with the radiation parameter (R_d) as well. Overall, the smaller the Biot number, the heat transfers from the surface to the fluid as portrayed at $y = 0.2$ and 0.3, while the larger the Biot number, the process of heat transfer reverses as depicted at $y = 0.4, 0.5, 0.7$.

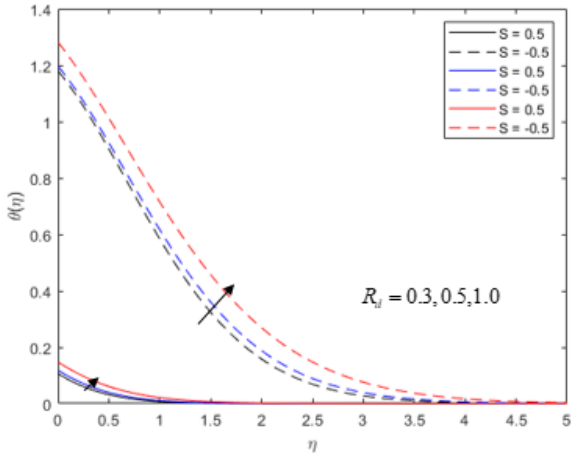

Fig. 14. Effects of Various Values of Radiation Parameter (R_d) on Temperature Profiles

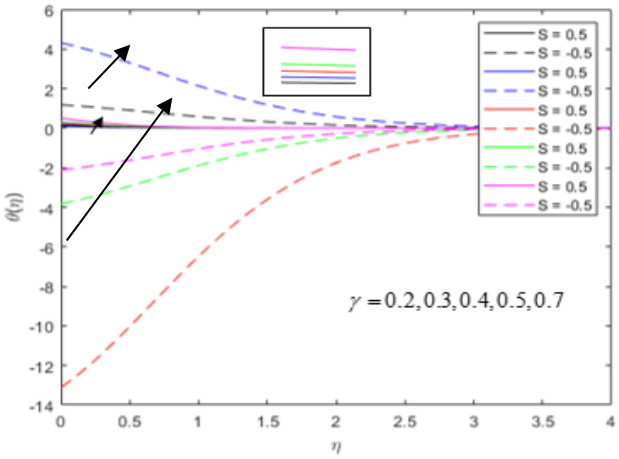

Fig. 15. Effects of Various Values of Biot Number (y) on Temperature

4. Conclusions

This study considers hybrid nanofluid with the suction/injection effects on the radiative flow of hyperbolic tangent liquid boundary layer. The rise in the values of volume fraction of both diamond (ϕ_1) and silicon dioxide (ϕ_2), power law index (n), Weissenberg number (We) for both suction and injection at 0.5 cases causes the increase of the velocity and decreasing of the skin friction coefficient. Meanwhile, with the increment of suction $(S > 0)$, the velocity profile decreases and vice versa for injection effect.

The temperature profile and the rate of heat transfer increase when the volume fraction of both diamond (ϕ_1), silicon dioxide (ϕ_2) for suction and radiation parameter (R_d) for both suction and injection. The temperature profile and the rate of heat transfer decrease when the power law index (n), Weissenberg number (We) increase for both suction and injection at 0.5 cases. Meanwhile, as the value of suction and injection vary increasingly, then the temperature profiles decrease. The smaller the Biot number (y), the heat transfers from the surface to the fluid, while the larger the Biot number, the process of heat transfer reverses the flow.

Nevertheless, this study holds great importance as a fundamental reference for a broad spectrum of nanofluid applications. The model presented in this research provides indispensable guidance for upcoming researchers, enabling them to develop more accurate and sophisticated models. Moreover, future advancements should focus on incorporating different types of nanoparticles and exploring various physical parameters to improve the model's accuracy and applicability. By continuously refining and expanding upon this study, we can uncover novel research pathways, leading to a deeper comprehension of nanofluid dynamics and sparking innovation and progress in this captivating field.

Acknowledgement
This research was funded by a grant from Universiti Teknologi Mara (UiTM) (600-RMC/GPK 5/3 (157/2020)).

References

[1] Oleinik, Olga Arsenievna, and Viacheslav Nikolaevich Samokhin. *Mathematical models in boundary layer theory*. Vol. 15. CRC Press, 1999.
[2] Rathore, Mahesh M., and R. Kapuno. *Engineering heat transfer*. Jones & Bartlett Publishers, 2010.
[3] Reddy, Nalivela Nagi, Vempati Srinivasa Rao, and B. Ravindra Reddy. "Chemical reaction impact on MHD natural convection flow through porous medium past an exponentially stretching sheet in presence of heat source/sink and viscous dissipation." *Case Studies in Thermal Engineering* 25 (2021): 100879. https://doi.org/10.1016/j.csite.2021.100879
[4] Megahed, Ahmed M., M. Gnaneswara Reddy, and W. Abbas. "Modeling of MHD fluid flow over an unsteady stretching sheet with thermal radiation, variable fluid properties and heat flux." *Mathematics and Computers in Simulation* 185 (2021): 583-593. https://doi.org/10.1016/j.matcom.2021.01.011
[5] Idowu, Amos S., and John O. Olabode. "Thermochemistry and viscous heat dissipative effects on unsteady upper-convected Maxwell fluid flow past a stretching vertical plate with thermophysical variables." *Heat Transfer* 50, no. 3 (2021): 2950-2974. https://doi.org/10.1002/htj.22013
[6] Waini, Iskandar, Anuar Ishak, and Ioan Pop. "Hybrid nanofluid flow towards a stagnation point on an exponentially stretching/shrinking vertical sheet with buoyancy effects." *International Journal of Numerical Methods for Heat & Fluid Flow* 31, no. 1 (2021): 216-235. https://doi.org/10.1108/HFF-02-2020-0086
[7] Ghazali, Nur Miza Syaheera, Khadijah Abdul Hamid, Siti Khuzaimah Soid, Ahmad Sukri Abd Aziz, and Zaileha Md Ali. "Stagnation point flow in nanofluids over a shrinking cylinder with slip effect and viscous dissipation." In *AIP Conference Proceedings*, vol. 2266, no. 1. AIP Publishing, 2020. https://doi.org/10.1063/5.0018062
[8] Shafiq, Anum, S. A. Lone, Tabassum Naz Sindhu, Q. M. Al-Mdallal, and G. Rasool. "Statistical modeling for bioconvective tangent hyperbolic nanofluid towards stretching surface with zero mass flux condition." *Scientific Reports* 11, no. 1 (2021): 13869. https://doi.org/10.1038/s41598-021-93329-y
[9] Ziaei-Rad, Masoud, Mahdi Saeedan, and Ebrahim Afshari. "Simulation and prediction of MHD dissipative nanofluid flow on a permeable stretching surface using artificial neural network." *Applied Thermal Engineering* 99 (2016): 373-382. https://doi.org/10.1016/j.applthermaleng.2016.01.063
[10] Choi, S. US, and Jeffrey A. Eastman. *Enhancing thermal conductivity of fluids with nanoparticles*. No. ANL/MSD/CP-84938; CONF-951135-29. Argonne National Lab.(ANL), Argonne, IL (United States), 1995.
[11] Wong, Kaufui V., and Omar De Leon. "Applications of nanofluids: current and future." *Advances in Mechanical Engineering* 2 (2010): 519659. https://doi.org/10.1155/2010/519659
[12] Pal, Dulal, and Gopinath Mandal. "Magnetohydrodynamic stagnation-point flow of Sisko nanofluid over a stretching sheet with suction." *Propulsion and Power Research* 9, no. 4 (2020): 408-422. https://doi.org/10.1016/j.jppr.2020.06.002
[13] Hayat, T., M. Ijaz Khan, M. Waqas, A. Alsaedi, and M. Farooq. "Numerical simulation for melting heat transfer and radiation effects in stagnation point flow of carbon-water nanofluid." *Computer Methods in Applied Mechanics and Engineering* 315 (2017): 1011-1024. https://doi.org/10.1016/j.cma.2016.11.033
[14] Ramzan, Muhammad, Mutaz Mohammad, Fares Howari, and Jae Dong Chung. "Entropy analysis of carbon nanotubes based nanofluid flow past a vertical cone with thermal radiation." *Entropy* 21, no. 7 (2019): 642. https://doi.org/10.3390/e21070642
[15] Soid, Siti Khuzaimah, Anuar Ishak, and Ioan Pop. "Boundary layer flow past a continuously moving thin needle in a nanofluid." *Applied Thermal Engineering* 114 (2017): 58-64. https://doi.org/10.1016/j.applthermaleng.2016.11.165
[16] Soid, Siti Khuzaimah, Anuar Ishak, and Ioan Pop. "MHD stagnation-point flow over a stretching/shrinking sheet in a micropolar fluid with a slip boundary." *Sains Malaysiana* 47, no. 11 (2018): 2907-2916. https://doi.org/10.17576/jsm-2018-4711-34
[17] Azmi, Nor Syazwani Mohd, Siti Khuzaimah Soid, Ahmad Sukri Abd Aziz, and Zaileha Md Ali. "Unsteady magnetohydrodynamics flow about a stagnation point on a stretching plate embedded in porous medium." In *Journal of Physics: Conference Series*, vol. 890, no. 1, p. 012013. IOP Publishing, 2017. https://doi.org/10.1088/1742-6596/890/1/012013
[18] Othman, Noor Adila, Nor Azizah Yacob, Norfifah Bachok, Anuar Ishak, and Ioan Pop. "Mixed convection boundary-layer stagnation point flow past a vertical stretching/shrinking surface in a nanofluid." *Applied Thermal Engineering* 115 (2017): 1412-1417. https://doi.org/10.1016/j.applthermaleng.2016.10.159
[19] Ghasemi, S. E., and Mohammad Hatami. "Solar radiation effects on MHD stagnation point flow and heat transfer of a nanofluid over a stretching sheet." *Case Studies in Thermal Engineering* 25 (2021): 100898. https://doi.org/10.1016/j.csite.2021.100898

[20] Alhamaly, A. S., Majid Khan, S. Z. Shuja, B. S. Yilbas, and Hussain Al-Qahtani. "Axisymmetric stagnation point flow on linearly stretching surfaces and heat transfer: Nanofluid with variable physical properties." *Case Studies in Thermal Engineering* 24 (2021): 100839. https://doi.org/10.1016/j.csite.2021.100839
[21] Mahmood, Zafar, Umar Khan, S. Saleem, Khadija Rafique, and Sayed M. Eldin. "Numerical analysis of ternary hybrid nanofluid flow over a stagnation region of stretching/shrinking curved surface with suction and lorentz force." *Journal of Magnetism and Magnetic Materials* 573 (2023): 170654. https://doi.org/10.1016/j.jmmm.2023.170654
[22] Makhdoum, Basim M., Zafar Mahmood, Umar Khan, Bandar M. Fadhl, Ilyas Khan, and Sayed M. Eldin. "Impact of suction with nanoparticles aggregation and joule heating on unsteady MHD stagnation point flow of nanofluids over horizontal cylinder." *Heliyon* 9, no. 4 (2023). https://doi.org/10.1016/j.heliyon.2023.e15012
[23] Zainal, Nurul Amira, Roslinda Nazar, Kohilavani Naganthran, and Ioan Pop. "Magnetic impact on the unsteady separated stagnation-point flow of hybrid nanofluid with viscous dissipation and Joule heating." *Mathematics* 10, no. 13 (2022): 2356. https://doi.org/10.3390/math10132356
[24] Norzawary, Nur Hazirah Adilla, Norfifah Bachok, and Fadzilah Md Ali. "Stagnation point flow over a stretching/shrinking sheet in a carbon nanotubes with suction/injection effects." *CFD Letters* 12, no. 2 (2020): 106-114.
[25] Sundar, L. Syam, Korada Viswanatha Sharma, Manoj K. Singh, and A. C. M. Sousa. "Hybrid nanofluids preparation, thermal properties, heat transfer and friction factor-a review." *Renewable and Sustainable Energy Reviews* 68 (2017): 185-198. https://doi.org/10.1016/j.rser.2016.09.108
[26] Bumataria, Rakesh K., N. K. Chavda, and Hitesh Panchal. "Current research aspects in mono and hybrid nanofluid based heat pipe technologies." *Heliyon* 5, no. 5 (2019). https://doi.org/10.1016/j.heliyon.2019.e01627
[27] Arani, Ali Akbar Abbasian, and Hossein Aberoumand. "Stagnation-point flow of Ag-CuO/water hybrid nanofluids over a permeable stretching/shrinking sheet with temporal stability analysis." *Powder Technology* 380 (2021): 152-163. https://doi.org/10.1016/j.powtec.2020.11.043
[28] Khan, Umair, A. Zaib, and A. Ishak. "Non-similarity solutions of radiative stagnation point flow of a hybrid nanofluid through a yawed cylinder with mixed convection." *Alexandria Engineering Journal* 60, no. 6 (2021): 5297-5309. https://doi.org/10.1016/j.aej.2021.04.057
[29] Gul, Taza, Basit Ali, Wajdi Alghamdi, Saleem Nasir, Anwar Saeed, Poom Kumam, Safyan Mukhtar, Wiyada Kumam, and Muhammad Jawad. "Mixed convection stagnation point flow of the blood based hybrid nanofluid around a rotating sphere." *Scientific Reports* 11, no. 1 (2021): 7460. https://doi.org/10.1038/s41598-021-86868-x
[30] Wahid, Nur Syahirah, Norihan Md Arifin, Najiyah Safwa Khashi'ie, Rusya Iryanti Yahaya, Ioan Pop, Norfifah Bachok, and Mohd Ezad Hafidz Hafidzuddin. "Three-dimensional radiative flow of hybrid nanofluid past a shrinking plate with suction." *Journal of Advanced Research in Fluid Mechanics and Thermal Sciences* 85, no. 1 (2021): 54-70. https://doi.org/10.37934/arfmts.85.1.5470
[31] Saupi, Suhaila, Aniza Abd Ghani, Norihan Md Arifin, Haliza Rosali, and Nur Syahirah Wahid. "An Exact Solution of MHD Hybrid Nanofluid over a Stretching Surface Embedded in Porous Medium in the Presence of Thermal Radiation and Slip with Suction." *CFD Letters* 15, no. 5 (2023): 74-85. https://doi.org/10.37934/cfdl.15.5.7485
[32] Khashi'Ie, Najiyah Safwa, Iskandar Waini, Nur Syahirah Wahid, Norihan Md Arifin, and Ioan Pop. "Radiative Hybrid Ferrofluid Flow Over a Permeable Shrinking Sheet in a Three-Dimensional System." *CFD Letters* 14, no. 11 (2022): 9-21. https://doi.org/10.37934/cfdl.14.11.921
[33] Zainal, Nurul Amira, Roslinda Nazar, Kohilavani Naganthran, and Ioan Pop. "Stability analysis of unsteady MHD rear stagnation point flow of hybrid nanofluid." *Mathematics* 9, no. 19 (2021): 2428. https://doi.org/10.3390/math9192428
[34] Rao, Singiresu S. *The finite element method in engineering*. Butterworth-Heinemann, 2017. https://doi.org/10.1016/B978-0-12-811768-2.00001-8
[35] Ghadikolaei, S. S., Kh Hosseinzadeh, Mohammad Hatami, and D. D. Ganji. "MHD boundary layer analysis for micropolar dusty fluid containing Hybrid nanoparticles (Cu-Al_2O_3) over a porous medium." *Journal of Molecular Liquids* 268 (2018): 813-823. https://doi.org/10.1016/j.molliq.2018.07.105
[36] Hayat, T., M. Ijaz Khan, M. Waqas, and A. Alsaedi. "Radiative flow of hyperbolic tangent liquid subject to Joule heating." *Results in Physics* 7 (2017): 2197-2203. https://doi.org/10.1016/j.rinp.2017.06.021
[37] Hayat, Tasawar, Sajid Qayyum, Ahmed Alsaedi, and Sabir Ali Shehzad. "Nonlinear thermal radiation aspects in stagnation point flow of tangent hyperbolic nanofluid with double diffusive convection." *Journal of Molecular Liquids* 223 (2016): 969-978. https://doi.org/10.1016/j.molliq.2016.08.102
[38] Nadeem, Sohail, and Safia Akram. "Magnetohydrodynamic peristaltic flow of a hyperbolic tangent fluid in a vertical asymmetric channel with heat transfer." *Acta Mechanica Sinica* 27 (2011): 237-250. https://doi.org/10.1007/s10409-011-0423-2

[39] Akbar, Noreen Sher, Sohail Nadeem, and Mohamed Ali. "Influence of heat and chemical reactions on hyperbolic tangent fluid model for blood flow through a tapered artery with a stenosis." *Heat Transfer Research* 43, no. 1 (2012). https://doi.org/10.1615/HeatTransRes.2012004295

[40] Khan, Muhammad Ijaz, Tasawar Hayat, Muhammad Waqas, and Ahmed Alsaedi. "Outcome for chemically reactive aspect in flow of tangent hyperbolic material." *Journal of Molecular Liquids* 230 (2017): 143-151. https://doi.org/10.1016/j.molliq.2017.01.016

[41] Ullah, Imran, Sharidan Shafie, and Ilyas Khan. "Effects of slip condition and Newtonian heating on MHD flow of Casson fluid over a nonlinearly stretching sheet saturated in a porous medium." *Journal of King Saud University-Science* 29, no. 2 (2017): 250-259. https://doi.org/10.1016/j.jksus.2016.05.003

[42] Ramzan, Muhammad, Naila Shaheen, Jae Dong Chung, Seifedine Kadry, Yu-Ming Chu, and Fares Howari. "Impact of Newtonian heating and Fourier and Fick's laws on a magnetohydrodynamic dusty Casson nanofluid flow with variable heat source/sink over a stretching cylinder." *Scientific Reports* 11, no. 1 (2021): 2357. https://doi.org/10.1038/s41598-021-81747-x

[43] Yusof, Nur Syamila, Siti Khuzaimah Soid, Mohd Rijal Illias, Ahmad Sukri Abd Aziz, and Nor Ain Azeany Mohd Nasir. "Radiative Boundary Layer Flow of Casson Fluid Over an Exponentially Permeable Slippery Riga Plate with Viscous Dissipation." *Journal of Advanced Research in Applied Sciences and Engineering Technology* 21, no. 1 (2020): 41-51. https://doi.org/10.37934/araset.21.1.4151

[44] Soid, Siti Khuzaimah, Anuar Ishak, and Ioan Pop. "MHD flow and heat transfer over a radially stretching/shrinking disk." *Chinese Journal of Physics* 56, no. 1 (2018): 58-66. https://doi.org/10.1016/j.cjph.2017.11.022

[45] Han, Anpan, Henrik Hartmann Henrichsen, Aleksei Savenko, Dirch Hjorth Petersen, and Ole Hansen. "Towards diamond micro four-point probes." *Micro and Nano Engineering* 5 (2019): 100037. https://doi.org/10.1016/j.mne.2019.05.002

[46] Usman, M., M. Hamid, T. Zubair, Rizwan Ul Haq, and Wei Wang. "Cu-Al2O3/Water hybrid nanofluid through a permeable surface in the presence of nonlinear radiation and variable thermal conductivity via LSM." *International Journal of Heat and Mass Transfer* 126 (2018): 1347-1356. https://doi.org/10.1016/j.ijheatmasstransfer.2018.06.005

[47] Khan, Arshad, Dolat Khan, Ilyas Khan, Farhad Ali, Faizan ul Karim, and Muhammad Imran. "MHD flow of sodium alginate-based Casson type nanofluid passing through a porous medium with Newtonian heating." *Scientific Reports* 8, no. 1 (2018): 8645. https://doi.org/10.1038/s41598-018-26994-1

[48] Mustafa, Meraj, Muhammad A. Farooq, Tasawar Hayat, and Ahmed Alsaedi. "Numerical and series solutions for stagnation-point flow of nanofluid over an exponentially stretching sheet." *Plos One* 8, no. 5 (2013): e61859. https://doi.org/10.1371/journal.pone.0061859